An Innovative Laser Metasurface Fabrication Technique for Highly Flexible Optoelectronic Devices

Qinghua Wang

Department of Mechanical Engineering, University of Iowa, Iowa City, IA 52242

Haoxuan You

Department of Mechanical Engineering, University of Iowa, Iowa City, IA 52242

Zach Lowery

Department of Mechanical Engineering, University of Iowa, Iowa City, IA 52242

Songwei Li

Department of Mechanical Engineering, University of Iowa, Iowa City, IA 52242

Hao Fu

Department of Mechanical Engineering, University of Iowa, Iowa City, IA 52242

Ruoxing Wang

School of Industrial Engineering, Purdue University, 315 N. Grant Street, West Lafayette, IN 47907

Caterina Lamuta

Department of Mechanical Engineering, University of Iowa, Iowa City, IA 52242

Fatima Toor

Department of Electrical & Computer Engineering, University of Iowa, Iowa City, IA 52242

Wenzhuo Wu

School of Industrial Engineering, Purdue University, 315 N. Grant Street, West Lafayette, IN 47907

Albert Ratner

Department of Mechanical Engineering, University of Iowa, Iowa City, IA 52242

Hongtao Ding¹

Department of Mechanical Engineering, University of Iowa, Iowa City, IA 52242 e-mail: hongtao-ding@uiowa.edu

Flexible optoelectronic devices have attracted considerable attention due to their low weight, portability, and ease of integration with other devices. However, major issues still exist: they are subject to repeated stresses, which often leads to damage; and the current fabrication methods such as photolithography and nanoimprint lithography can be very time-consuming or costly. This work aims to develop a novel cost-effective and time-efficient laser metasurface fabrication (LMF) technique for production of flexible optoelectronic devices. The experimental results have shown that the laser patterned flexible surfaces exhibit high visible transmittance, low sheet resistance, and extraordinary mechanical durability under repeated bending cycles. The laser patterned flexible surfaces have also demonstrated the potential to be utilized as heaters, which renders them new de-icing or defogging applications. This innovative laser patterning method will provide a new avenue for fabrication of multifunctional optoelectronic devices. [DOI: 10.1115/1.4046032]

Keywords: laser surface patterning, flexible optoelectronic device, mechanically durable, heater

1 Introduction

Transparent conductors are an integral component in many optoelectronic devices (ODs), such as displays, light-emitting diodes (LEDs), touch screen panels, smart windows, and solar cells [1-6]. In recent years, there is a growing research need for development of flexible transparent conductors (FTCs), which is considered as a key component for the next-generation ODs. The FTCs have many advantages including weight saving, good portability, and ease of integration with other devices. The FTCs can be utilized for various applications, such as transparent conductive heater [7-8], electromagnetic inference shielding [9,10], electronic skin (E-skin) [11,12], and organic light-emitting diode [2,4]. The global market for FTCs is forecast to grow by nearly 10 times to U.S. dollar (USD) 16.50 billion by 2021 [13]. However, there are two major issues associated with the FTCs: (1) they are subject to repeated stress, which often leads to damage and cracks. There exists an urgent need to enhance the reliability and durability of the electrode component in FTCs and (2) the state-of-art fabrication methods for the FTCs are either too time-consuming or costly, which has posed challenges for development of innovative time-efficient and cost-effective fabrication methods.

In order to fabricate high quality FTCs, many different fabrication techniques have been used, including direct laser surface pattering [14-19], electrospinning [20,21], and inkjet printing [22,23]. Among all these fabrication methods, direct laser surface patterning is rapidly gaining its popularity due to the advantages of relatively low cost, environmental friendliness, process flexibility, and ease of automation [14-19]. However, there are several major issues associated with the state-of-art laser surface patterning techniques for fabrication of FTCs. First, existing laser surface patterning methods usually take too long to process a unit area (e.g., ~two hours to process the FTC with a surface area of 1 in. × 1 in.), which will make it very difficult to scale up the process. Second, the laser-patterned surface typically exhibits good electrical conductivity and optical response in visible spectrum only, which have tremendously restricted their applications in diverse areas [14,15,17]. New material processing science is essentially needed to fabricate optoelectronic device that can function in various electromagnetic spectra, e.g., visible and terahertz (THz) spectra. Therefore, a time-efficient laser-based

¹Corresponding author.

Contributed by the Manufacturing Engineering Division of ASME for publication in the JOURNAL OF MICRO- AND NANO-MANUFACTURING. Manuscript received October 12, 2019; final manuscript received January 1, 2020; published online February 13, 2020. Assoc. Editor: Lawrence Kulinsky.

manufacturing technique is essentially needed for development and fabrication of multifunctional FTCs.

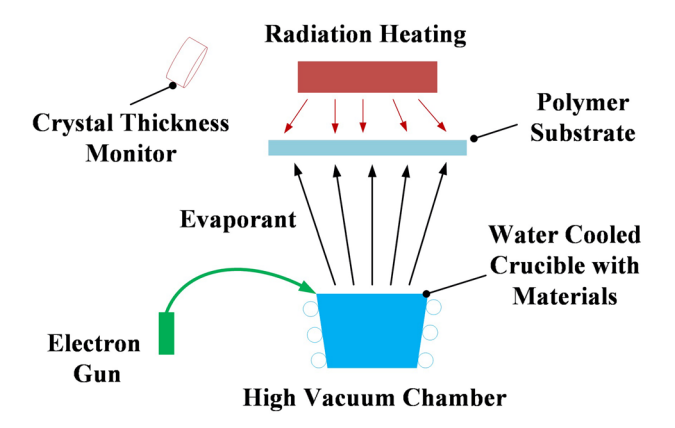
The authors' research group has previously developed an innovative laser metasurface fabrication (LMF) method for production of multifunctional optoelectronic devices on transparent dielectric substrates such as quartz and soda-lime glass. The LMF surface not only shows good electrical conductivity and high visible transparency but also exhibits self-tunable bandpass filtering effect in THz domain [24–26]. In this work, the LMF process was applied to flexible dielectric substrates, e.g., polyethylene terephthalate (PET) and Ecoflex, and has rendered new surface functionalities. The LMF process shows its effectiveness for fabrication of highly mechanically durable FTCs and resolves the problems of material cost and manufacturing complexity. This innovative technique could have a tremendous impact for the optoelectronic device manufacturers.

2 Experiments

2.1 Ultra-Thin Metal Film Deposition. Two different flexible substrates, PET and Ecoflex, were used in this research work. PET is a type of general-purpose thermoplastic polymer, which has been widely used for fabrication of optoelectronic devices [9,27]. Biaxially oriented PET purchased from Goodfellow Corporation is used in this work due to its high tensile strength, and chemical and dimensional stability. Ecoflex is rubber-like thin film, which also shows great potential as substrate material for optoelectronic devices [28-30]. Compared with PET, Ecoflex is more bendable and stretchable, and thus the transparent conducting electrodes fabricated on top of it tend to exhibit better mechanical durability. Although Ecoflex should be considered as the ideal substrate for flexible optoelectronic devices, there has been limited research that employs Ecoflex for device fabrication. Thus, it will be of particular interest to further investigate the performance of Ecoflex when used as the substrate of optoelectronic devices. In this work, the PET substrate has a thickness of 250 μ m and the Ecoflex substrate has a thickness of $500 \, \mu m$. Before the thin film deposition, each substrate was ultrasonically cleaned using a sequence of baths containing acetone, isopropyl alcohol, and distilled water to remove any contaminations on the substrates. An ultrathin copper (Cu) film with a thickness of \sim 9 nm was then deposited onto these two different substrates using electron-beam physical vapor deposition.

2.2 Laser Metasurface Fabrication. Laser metasurface fabrication process consists of two steps: first, an ultrathin metal film is deposited onto the flexible dielectric substrate as described in Sec. 2.1; second, the ultrathin metal film is laser patterned with periodic hole array structure to achieve combined optoelectronic functions [24,25]. The schematic of LMF process is shown in Fig. 1. The laser patterning experiments utilize a laser scanning system including a 1,064 nm wavelength Q-Switched Nd:YAG nanosecond laser and a three-axis galvanometer laser scanner (SCANLAB intelliSCAN® 20 and varioSCANde 40i, Puchheim, Germany). The laser scanner is configured with an f-theta objective and serves to direct the laser beam onto the ultrathin metal film. The flexible substrates used in this work are highly transparent at this laser wavelength and thus does not absorb laser energy. This nanosecond laser patterning method could enable efficient material removal without inducing thermal damage on the underlying flexible substrates. The laser processing parameters, e.g., scanning speed and pitch (y-direction distance between each scanning line) were adjusted by the control software. Each laser patterned sample has a surface area of 1 in. × 1 in. Compared with the existing laser patterning techniques for optoelectronic device fabrication [14,15,17], the LMF process increases the laser processing rate by at least two orders, which will enable large-area processing of optoelectronic device for practical throughput. The LMF surface also exhibits both high visible transparency and bandpass filtering effect in THz region, which will greatly expand the applications of the process. It should be noted that the THz

Step 1: Ultrathin Metal Film Deposition



Step 2: Laser Surface Patterning

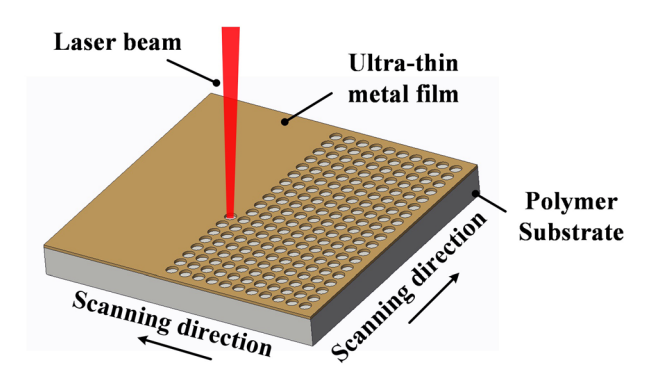


Fig. 1 Schematic of the LMF process

bandpass filtering effect of LMF surface has been presented previously by the authors' group but is beyond the scope of this work [25,26]. Therefore, the THz bandpass filtering effect will not be discussed here.

2.3 Surface Characterization Tests. Three-dimensional (3D) surface profile of the flexible LMF surface was measured using a Wyko NT1000 3D optical profiling system and microstructure of the flexible LMF surface was captured using a Hitachi S-4800 scanning electron microscope. Sheet resistance of the flexible LMF surface was tested with a digital four-point probe sheet resistivity measurement system (Signatone Pro4 series), which is connected to a source meter (Keithley 2400 series) for reading the sheet resistance values. Optical transmittance of the flexible LMF surfaces was measured using a UV–Vis spectrometer (USB4000, Ocean Optics, Co.). Oceanview software was used to process and visualize the optical transmittance measurement results.

Cyclic bending tests were conducted using a TestResources tensile test machine to evaluate the mechanical durability of the flexible LMF surfaces under repeated fatigue bending cycles. Before the test, each flexible LMF surface was properly secured on the test machine. During the cyclic bending tests, one end of the LMF surface was fixed while the other end was cycled at a frequency of 2 Hz. The real-time sheet resistance of the flexible LMF surfaces was recorded at every 200 repeated bending cycles until the completion of 1400 cycles. The heating performance of the flexible LMF surfaces was characterized using an infrared (IR) camera (FLIR Systems, Inc., Wilsonville, OR) at room temperature. Before the temperature measurement, the flexible LMF surfaces were sprayed with a thin layer of enamel paint (with a calibrated emissivity of ~0.96) to eliminate the reflection [31]. During the

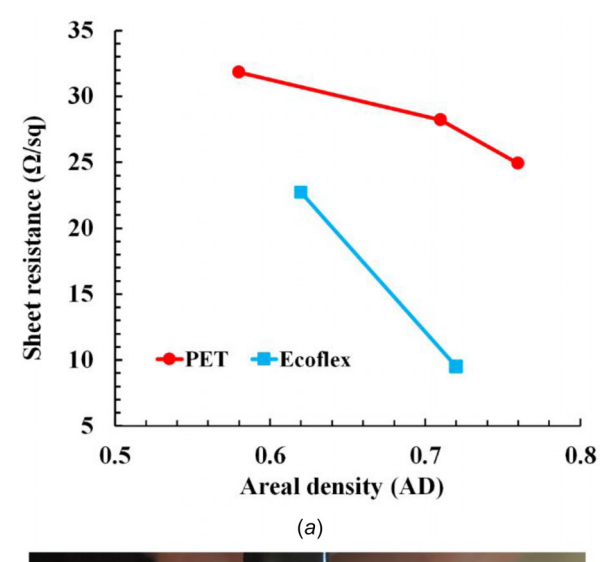
temperature measurement, different direct current (DC) voltages ranging from 2 V to 12 V, with an increment of 2 V, were applied to the top surface of the LMF surface. The average temperature profile and IR thermal images were recorded by the IR camera to evaluate the heating performance of the flexible LMF surfaces. The maximum voltage applied is 12 V, since the flexible LMF surface tends to get cracked and damaged when using a voltage higher than $12\,\rm V$.

3 Results and Discussions

3.1 Sheet Resistance. The sheet resistance of the flexible LMF surfaces, fabricated on PET and Ecoflex substrates, is shown in Fig. 2(a). Based on the experimental results, it can be found that area density (AD), defined as the ratio of the residual area after LMF process over the total area, plays a key role for the sheet resistance of the flexible LMF surfaces. For the LMF surfaces with PET as substrate, as the AD of the LMF surface increased from 58% to 76%, the sheet resistance decreased from 31.8 Ω /sq to 24.9 Ω /sq. For the LMF surface with Ecoflex as substrate, as the AD of the LMF surface increased from 62% to 72%, the sheet resistance decreased from 22.7 Ω /sq to 9.5 Ω /sq. The sheet resistance of the LMF surfaces, using both flexible substrates, has increased compared with that of the untreated 9 nm-thick Cu film $(\sim 8 \Omega/\text{sq})$. This is mainly attributed to a significant amount of Cu film removed by the LMF process, which decreases the area for electrical current to pass through, thus resulting in a higher sheet resistance [24,25]. Nevertheless, the increase of sheet resistance on the LMF surface is still within a reasonable range. It can be found in Fig. 2(b) that the flexible LMF surface can be used to provide electrical connection for LED indicator. The ultrathin transparent conducting metal film with a sheet resistance on the order of \sim 25–30 Ω /sq is comparable to other transparent conducting metal oxide, such as indium tin oxide (ITO) and aluminiumdoped zinc oxide (AZO). Therefore, the flexible LMF surfaces fabricated in this work have good potential to be utilized in various optoelectronic devices and applications.

3.2 Optical Transmittance. The optical transmittance of the LMF surfaces was significantly enhanced compared with that of the untreated 9 nm-thick Cu film. Previous research work has demonstrated the importance of selecting a reasonable thickness for ultrathin metal film [24,25]. It is generally accepted that a semi-transparent ultrathin metal film should be used to achieve a good balance between the sheet resistance and visible transmittance of the LMF surface, due to the fact that these two properties are contradicting [32]. In this work, the thickness of the ultrathin Cu film was set at 9 nm, which was found to be effective for balancing the two optoelectronic properties of the LMF surfaces. As shown in Fig. 3, the untreated 9 nm-thick Cu films deposited on the PET and Ecoflex substrates had an optical transmittance of 40.8% and 53.0%, respectively. The difference between the optical transmittance of the untreated Cu films on these two substrates is mainly due to the difference in thickness between the two substrates, which has led to the slight difference of the deposited Cu film thickness. After laser surface patterning, the optical transmittance of the LMF surfaces using PET and Ecoflex as substrate was increased to 59.9% and 62.5%, respectively, using the optimal AD values. It can be found that the LMF surface could have a combined optical transmittance of ~60% and sheet resistance of \sim 20 Ω /sq using both flexible substrates. It is believed the AD value can be further adjusted in order to optimize the optoelectronic performance of the LMF surfaces. The experimental results have demonstrated the potential of the LMF process as an efficient manufacturing technique for fabrication of flexible optoelectronic devices.

The two-dimensional optical image, scanning electron microscope (SEM) image of a single-shot laser spot, and 3D surface profile of the flexible LMF surface using Ecoflex as the substrate material are shown in Figs. 4(a)-4(c), respectively. Based on the



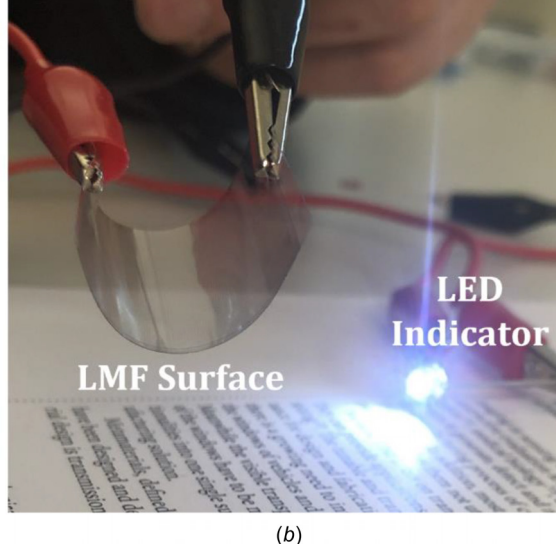


Fig. 2 Sheet resistance of the flexible LMF samples on PET and Ecoflex substrates: (a) sheet resistance as a function of AD and (b) photograph of a LMF surface showing that it can be used to provide electrical connection for LED indicator

optical and SEM images as well as the 3D surface profile, it can be found that a high-quality microhole array pattern was developed on the ultrathin, 9 nm-thick Cu film. It can be clearly found from these images that the whole laser patterned area is free of cracks and delaminations demonstrating the effectiveness of the LMF process for fabricating high-quality transparent conducting surface. The laser patterned microholes, with a feature size of \sim 150 μ m, appear to be circular and periodically arrayed. However, some burrs have been generated at the periphery of each hole as a result of relatively high laser fluence, which has led to melt surface instability and expulsion during the LMF process [24,25]. It should be noted that these burrs are neither visibly transparent nor electrically conductive and have increased the surface roughness. These problems might contribute to the imperfect combined optoelectronic properties of the LMF surfaces. Therefore, there is still room for further improvement of surface quality of the flexible LMF surfaces.

3.3 Fatigue Bending Performance. The fatigue bending performance of the flexible LMF surfaces was examined via cyclic bending tests conducted using a tensile test machine. As shown in Fig. 5(*a*), both ends of the flexible LMF surface were properly secured on the tensile test machine first. After the test started, the

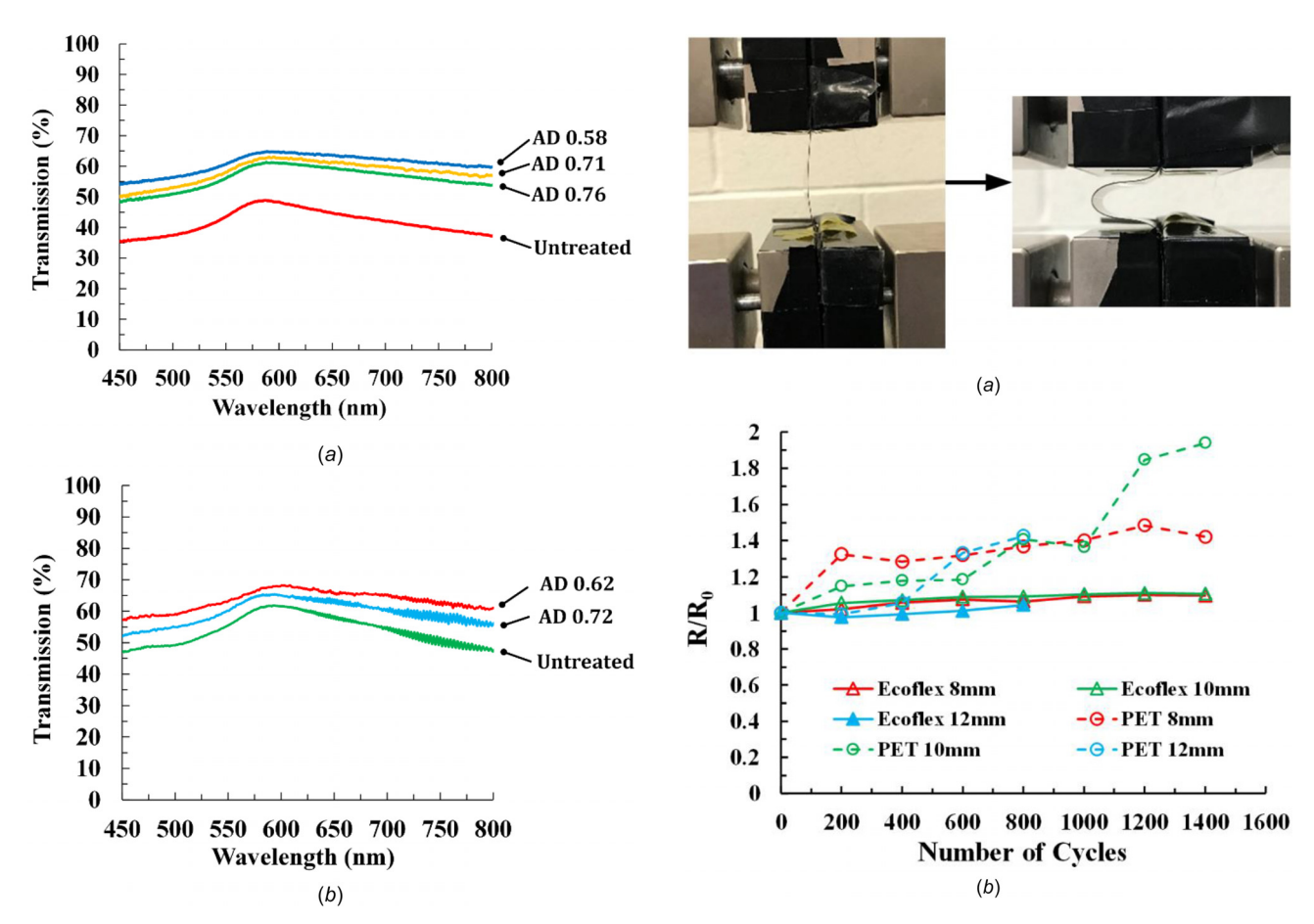


Fig. 3 Optical transmittance of LMF surfaces: (a) PET substrate and (b) Ecoflex substrate

LMF surface was stretched and compressed back and forth at a frequency of $2\,\mathrm{Hz}$. The real-time sheet resistance of the flexible LMF surfaces was recorded at every 200 repeated bending cycles. In this section, a comprehensive experimental study was carried out to evaluate the effects of substrate material and adhesion layer on the mechanical durability of the LMF surfaces. First, cyclic bending tests were conducted on the flexible LMF surfaces with PET and Ecoflex as substrate materials to investigate how substrate material affects the fatigue bending performance. Three different bending radius values were used in the bending tests: $8\,\mathrm{mm}$, $10\,\mathrm{mm}$, and $12\,\mathrm{mm}$. The bending radius r_b was calculated using Eq. (1) [22]

$$r_b = \frac{L}{2\pi\sqrt{\frac{dL}{L} - \frac{\pi^2 t_s^2}{12L^2}}} \tag{1}$$

Fig. 5 Fatigue bending performance of LMF surface: (a) experimental demonstration of cyclic bending test and (b) ratio of the real-time sheet resistance over the initial sheet resistance for the flexible LMF surfaces with different substrate materials when bended using multiple bending radius values

where L represents the initial length of the LMF surface, dL/L represents the change rate of the length, and t_s represents the thickness of the substrate. Fig. 5(b) shows the ratio of the real-time sheet resistance, R, over the initial sheet resistance, R_0 , for the flexible LMF surfaces with different substrate materials when bended using different bending radius values. Throughout 1400 bending cycles, the change of sheet resistance was within 10% of its original value for the LMF surface with Ecoflex as the substrate material. Nevertheless, the change of sheet resistance was much larger for the LMF surfaces with PET as the substrate material. The change in sheet resistance during the cyclic bending test is believed to arise from the cracks and the increased contact

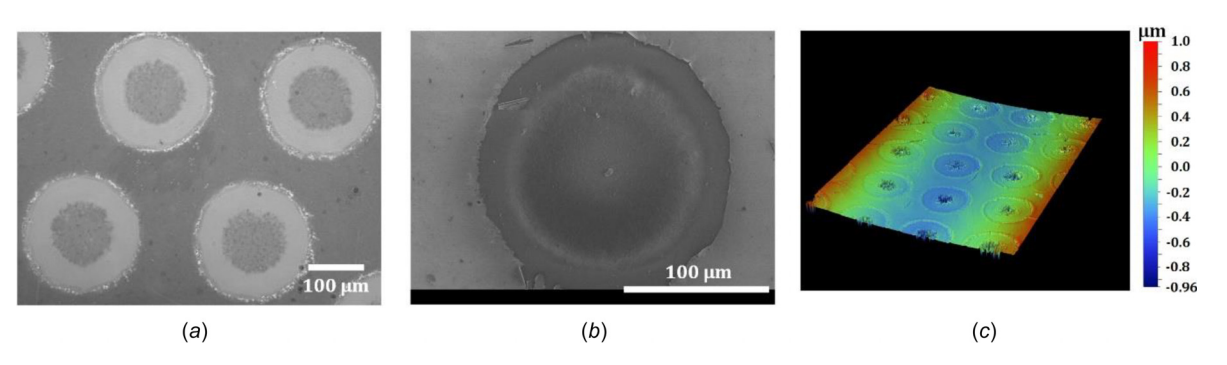


Fig. 4 LMF surface pattern with an area density of 72%: (a) optical image, (b) SEM image of a single-shot laser spot, and (c) 3D surface profile

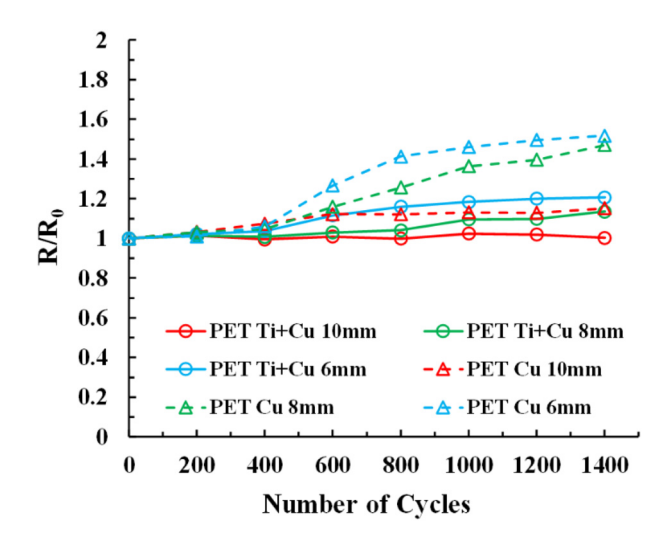


Fig. 6 Effect of adhesion layer on the fatigue bending performance of the PET-based LMF surfaces when bended using different bending radius values

resistance between the laser patterned Cu film and the substrate [15,16]. Therefore, the minimal change of R/R_0 value when using Ecoflex as substrate indicates that very few cracks were generated during the cyclic bending tests and thus the increase of contact resistance was well restricted. This shows that Ecoflex is an ideal substrate material which can promote the mechanical durability of flexible LMF surface under repeated bending conditions due to its superior bendability and stretchability. Ecoflex is also highly compatible with the LMF process, and this has demonstrated the huge potential of the LMF process coupled with Ecoflex to be widely utilized for fabrication of the next-generation flexible optoelectronic devices.

It is found that the flexible LMF surfaces with PET as the substrate material did not exhibit satisfying fatigue bending performance compared with those using Ecoflex as the substrate material, as shown in Fig. 5(b). This could be attributed to the fact that PET is less bendable and stretchable than Ecoflex. Therefore, more cracks can be generated and the contact resistance will increase more rapidly during the cyclic bending test. However, previous research has shown that PET is a key and widely used substrate material in the modern flexible electronics industries [5,33,34]. Therefore, further study was conducted on the PET-based flexible LMF surfaces to evaluate how their fatigue bending performance can be further enhanced. Some researchers used titanium (Ti) layer to promote the adhesion between the polymer substrates and the Cu or gold (Au) conducting lines, and the experimental results demonstrated that good adhesion of conducting lines was achieved, which are critical for the performance and lifetime of flexible electronics [35,36]. In this work, Ti adhesion layer was also used to demonstrate its effectiveness for enhancing the mechanical durability of the PET-based flexible LMF surfaces. Figure 6 shows the R/R_0 values of the PET-based flexible LMF surfaces with and without Ti adhesion layer when bended using the bending radius values of 6 mm, 8 mm, and 10 mm. It is found that without Ti adhesion layer, the R/R_0 value increased rapidly only after a few hundred bending cycles. However, by inserting a Ti adhesion layer between the PET substrate and Cu film, the change of sheet resistance was within 20% of its original value even using a bending radius as low as 6 mm. This clearly indicates the importance and effectiveness of adhesion layer on enhancing the fatigue bending performance of the PET-based LMF surfaces. The use of adhesion layer has effectively promoted the bonding strength between the substrate and the ultrathin Cu film, and led to fewer cracks and limited the increase of contact resistance. This adhesion layer-assisted method has provided another highly efficient path for enhancing the mechanical durability of the flexible

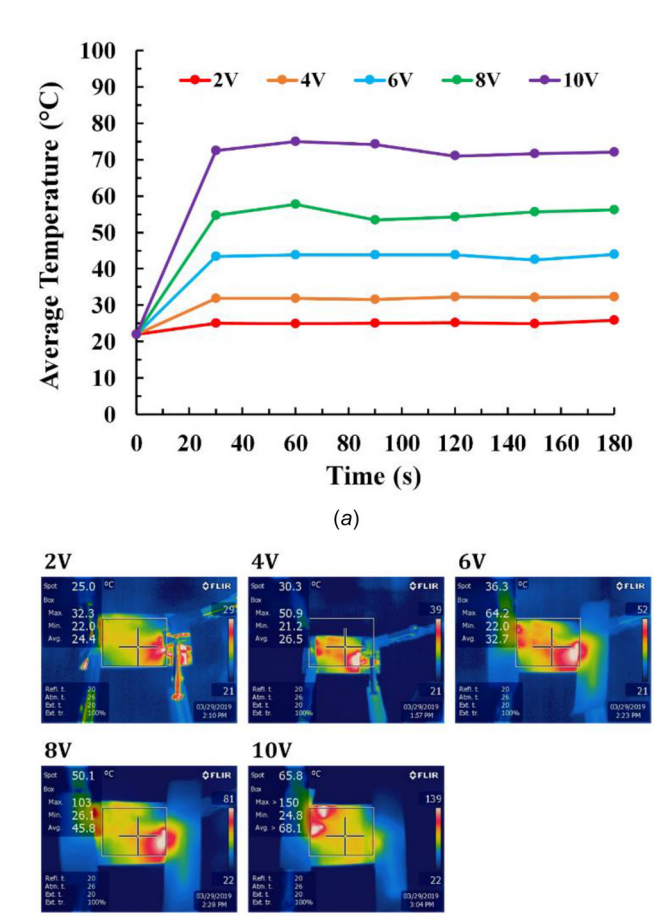


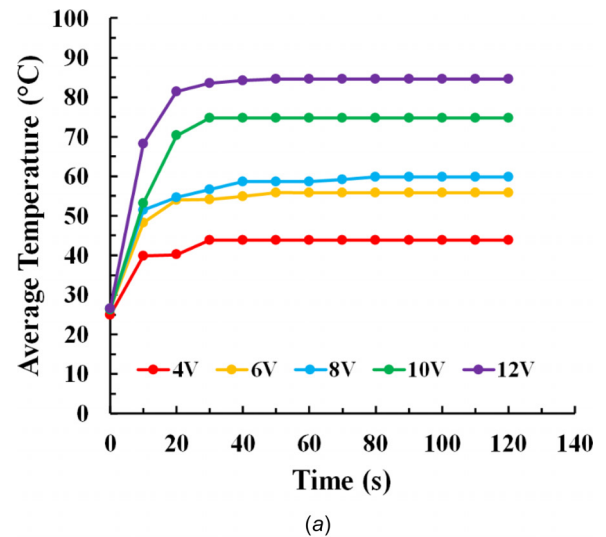
Fig. 7 Infrared temperature measurement of LMF-built Ecoflex sample at various electrical loadings: (a) average surface temperature histories at different external voltages and (b) IR thermal images after applying voltages for 30 s

(b)

LMF surfaces, and makes the LMF process applicable to more flexible substrate materials.

3.4 Heating Performance. The heating performance of the flexible LMF surface was evaluated to demonstrate its potential to be utilized as a heater. Figure 7(a) shows the evolution of the average surface temperature in terms of time at different external voltages. The heating tests were conducted at the room temperature of 25 °C. Figure 7(b) shows the IR thermal images, which clearly demonstrates the temperature distributions of the LMF surface patterned on Ecoflex after applying different external voltages for 30 s. It can be found that the average surface temperature on the LMF surface exhibits distinct increase as the applied external voltage becomes larger. With an external voltage of 10 V, the average surface temperature rapidly increased to ~75 °C in 30 s and maintained at this stable value afterward. As shown in the IR thermal images, the temperature distribution on the flexible LMF surfaces is quite uniform except for a small area on the corners, which could be attributed to the imperfect electrode connection during the thermal experiments. It is believed that the uniform hole array pattern, as shown in Fig. 4, has guaranteed the efficient conversion of electrical energy into heat energy for the flexible LMF surfaces. The exceptional heating performance of the LMF surfaces will make them a strong candidate for various applications, such as anti-icing and anti-fogging windows, which will eventually benefit the automobile and aerospace industries.

The heating performance of the PET-based LMF surfaces with Ti adhesion layer was evaluated using the same measurement method. It is well known that Ti has much lower thermal



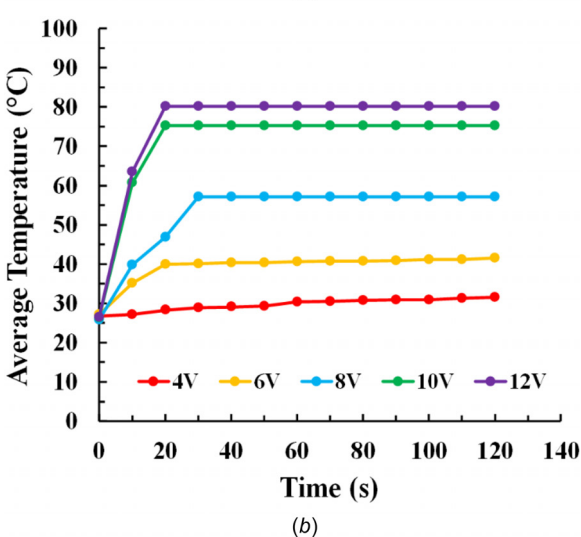


Fig. 8 Average surface temperature profiles for the PET-based LMF surface at different external voltages: (a) without adhesion layer and (b) with adhesion layer

conductivity compared with Cu [37]. Therefore, the aim of the temperature measurement for the PET-based LMF surfaces with and without adhesion layer is to examine whether the heating performance will be significantly degraded by adding the Ti adhesion layer. As shown in Fig. 8(a), the average surface temperature of the PET-based LMF surface without Ti adhesion layer rapidly increased to ~85 °C within 30 s and the temperature value became stable afterward at an external voltage of 10 V. Interestingly, it is found that the average surface temperature of the PET-based LMF surface with Ti-adhesion layer increased to ~80 °C within 30 s at the same external voltage as shown in Fig. 8(b), demonstrating that the heating performance of the PET-based LMF surfaces was not significantly affected by the use of adhesion layer. The experimental results clearly indicate that the mechanical durability of the flexible LMF surface can be significantly enhanced using adhesion layer, while its potential to be used as a heater is well preserved. This adhesion layer-assisted method is considered as highly promising for enhancement of the overall mechanical and heating functionalities of the flexible LMF surface.

4 Conclusions

An innovative LMF method was developed and used in this work for fabrication of flexible transparent conductors. The

flexible LMF surfaces exhibit exceptional combined surface functions of high visible transmittance, good electrical conductivity, and outstanding mechanical durability. It is also demonstrated that the surface temperature of the flexible LMF surfaces increases rapidly with external voltage applied, which makes them good candidates to be applied as a heater for anti-icing or anti-fogging applications. This innovative LMF process has strong potential to provide a new manufacturing avenue for the next generation of flexible optoelectronic devices.

Funding Data

 University of Iowa by the National Science Foundation (Grant No. 1762353; Funder ID: 10.13039/100008893).

References

- Shin, Y. H., Cho, C. K., and Kim, H. K., 2013, "Resistance and Transparency Tunable Ag-Inserted Transparent InZnO Films for Capacitive Touch Screen Panels," Thin Solid Films, 548, pp. 641–645.
- [2] Triambulo, R. E., Cheong, H. G., and Park, J. W., 2014, "All-Solution-Processed Foldable Transparent Electrodes of Ag Nanowire Mesh and Metal Matrix Films for Flexible Electronics," Org. Electron. Phys., Mater. Appl., 15(11), pp. 2685–2695.
- [3] Hssein, M., Tuo, S., Benayoun, S., Cattin, L., Morsli, M., Mouchaal, Y., Addou, M., Khelil, A., and Bernède, J. C., 2017, "Cu-Ag Bi-Layer Films in Dielectric/Metal/Dielectric Transparent Electrodes as ITO Free Electrode in Organic Photovoltaic Devices," Org. Electron. Phys., Mater. Appl., 42, pp. 173–180.
- [4] Ye, T., Jun, L., Kun, L., Hu, W., Ping, C., Ya-Hui, D., Zheng, C., Yun-Fei, L., Hao-Ran, W., and Yu, D., 2017, "Inkjet-Printed Ag Grid Combined With Ag Nanowires to Form a Transparent Hybrid Electrode for Organic Electronics," Org. Electron. Phys., Mater. Appl., 41, pp. 179–185.
- [5] Formica, N., Sundar Ghosh, D., Chen, T. L., Eickhoff, C., Bruder, I., and Pruneri, V., 2012, "Highly Stable Ag-Ni Based Transparent Electrodes on PET Substrates for Flexible Organic Solar Cells," Sol. Energy Mater. Sol. Cells, 107, pp. 63–68.
- [6] Kato, Y., Jung, M. C., Lee, M. V., and Qi, Y., 2014, "Electrical and Optical Properties of Transparent Flexible Electrodes: Effects of UV Ozone and Oxygen Plasma Treatments," Org. Electron. Phys., Mater. Appl., 15(3), pp. 721–728.
- [7] Li, P., Ma, J. G., Xu, H. Y., Lin, D., Xue, X. D., Yan, X. Z., Xia, P., and Liu, Y. C., 2016, "Flexible Transparent Heaters Based on Silver Nanotrough Meshes," J. Alloys Compd., 664, pp. 764–769.
- [8] Lim, M., Kim, H. J., Ko, E. H., Choi, J., and Kim, H. K., 2016, "Ultrafast Laser-Assisted Selective Removal of Self-Assembled Ag Network Electrodes for Flexible and Transparent Film Heaters," J. Alloys Compd., 688, pp. 198–205.
- [9] Hu, M., Gao, J., Dong, Y., Li, K., Shan, G., Yang, S., and Li, R. K. Y., 2012, "Flexible Transparent PES/Silver Nanowires/PET Sandwich-Structured Film for High-Efficiency Electromagnetic Interference Shielding," Langmuir, 28(18), pp. 7101–7106.
- [10] Han, J., Wang, X., Qiu, Y., Zhu, J., and Hu, P., 2015, "Infrared-Transparent Films Based on Conductive Graphene Network Fabrics for Electromagnetic Shielding," Carbon N. Y., 87(C), pp. 206–214.
- [11] Lyu, H., Ping, X., Gao, R., Xu, L., and Pan, L., 2017, "Transparent Electronic Skin Device Based on Microstructured Silver Nanowire Transparent Electronic Skin Device Based on Microstructured Silver Nanowire Electrode," Chin. J. Chem. Phys., 30(5), pp. 603–608.
- [12] Wang, Q., Jian, M., Wang, C., and Zhang, Y., 2017, "Carbonized Silk Nanofiber Membrane for Transparent and Sensitive Electronic Skin," Adv. Funct. Mater., 27(9), pp. 1–9.
- [13] Banks, M., 2010, "Flexible Electronics Enters the E-Reader Market," Phys. World, 23(2), p. 8.
- [14] Han, S., Hong, S., Ham, J., Yeo, J., Lee, J., Kang, B., Lee, P., Kwon, J., Lee, S. S., Yang, M. Y., and Ko, S. H., 2014, "Fast Plasmonic Laser Nanowelding for a Cu-Nanowire Percolation Network for Flexible Transparent Conductors and Stretchable Electronics," Adv. Mater., 26(33), pp. 5808–5814.
- [15] Hong, S., Yeo, J., Kim, G., Kim, D., Lee, H., Kwon, J., Lee, H., Lee, P., and Ko, S. H., 2013, "Nonvacuum, Maskless Fabrication of a Flexible Metal Grid Transparent Conductor by Low-Temperature Selective Laser Sintering of Nanoparticle Ink," ACS Nano, 7(6), pp. 5024–5031.
- [16] Kang, Z., Wu, B., Wang, R., and Wu, W., 2018, "Laser-Based Fabrication of Carbon Nanotube–Silver Composites With Enhanced Fatigue Performance Onto a Flexible Substrate," ASME J. Manuf. Sci. Eng., 140(9), p. 091005.
- [17] Paeng, D., Yoo, J. H., Yeo, J., Lee, D., Kim, E., Ko, S. H., and Grigoropoulos, C. P., 2015, "Low-Cost Facile Fabrication of Flexible Transparent Copper Electrodes by Nanosecond Laser Ablation," Adv. Mater., 27(17), pp. 2762–2767.
- [18] Lee, D., Paeng, D., Park, H. K., and Grigoropoulos, C. P., 2014, "Vacuum-Free, Maskless Patterning of Ni Electrodes by Laser Reductive Sintering of Nio Nanoparticle Ink and Its Application to Transparent Conductors," ACS Nano, 8(10), pp. 9807–9814.

- [19] Theuring, M., Steenhoff, V., Geißendörfer, S., Vehse, M., von Maydell, K., and Agert, C., 2015, "Laser Perforated Ultrathin Metal Films for Transparent Electrode Applications," Opt. Express, 23(7), p. A254.
- [20] Wu, H., Kong, D., Ruan, Z., Hsu, P.-C., Wang, S., Yu, Z., Carney, T. J., Hu, L., Fan, S., and Cui, Y., 2013, "A Transparent Electrode Based on a Metal Nanotrough Network," Nat. Nanotechnol., 8(6), pp. 421–425.
 [21] Hsu, P. C., Kong, D., Wang, S., Wang, H., Welch, A. J., Wu, H., and Cui, Y.,
- [21] Hsu, P. C., Kong, D., Wang, S., Wang, H., Welch, A. J., Wu, H., and Cui, Y., 2014, "Electrolessly Deposited Electrospun Metal Nanowire Transparent Electrodes," J. Am. Chem. Soc., 136(30), pp. 10593–10596.
- [22] Yang, S. M., Lee, Y. S., Jang, Y., Byun, D., and Choa, S. H., 2016, "Electromechanical Reliability of a Flexible Metal-Grid Transparent Electrode Prepared by Electrohydrodynamic (EHD) Jet Printing," Microelectron. Reliab., 65, pp. 151–159.
- [23] Jeong, J. A., Kim, H. K., and Kim, J., 2014, "Invisible Ag Grid Embedded With ITO Nanoparticle Layer as a Transparent Hybrid Electrode," Sol. Energy Mater. Sol. Cells, 125, pp. 113–119.
- [24] Wang, Q., Li, B., Toor, F., and Ding, H., 2019, "Novel Laser-Based Metasur-face Fabrication Process for Transparent Conducting Surfaces," J. Laser Appl., 31(2), p. 022505.
- [25] Wang, Q., Raglione, M., Li, B., Jin, X., Toor, F., Arnold, M., and Ding, H., 2019, "High Throughput Laser Process of Transparent Conducting Surfaces for Terahertz Bandpass Ultrathin Metamaterials," Sci. Rep., 9(1), p. 3083.
- [26] Wang, Q., Gao, B., Raglione, M., Wang, H., Li, B., Toor, F., Arnold, M. A., and Ding, H., 2019, "Design, Fabrication, and Modulation of THz Bandpass Metamaterials," Laser Photon. Rev., 13(11), p. 1900071.
- [27] Hong, S. Y., Lee, Y. H., Park, H., Jin, S. W., Jeong, Y. R., Yun, J., You, I., Zi, G., and Ha, J. S., 2016, "Stretchable Active Matrix Temperature Sensor Array of Polyaniline Nanofibers for Electronic Skin," Adv. Mater., 28(5), pp. 930–935.
- aniline Nanofibers for Electronic Skin," Adv. Mater., 28(5), pp. 930–935.
 [28] Woo, J. Y., Kim, K. K., Lee, J., Kim, J. T., and Han, C. S., 2014, "Highly Conductive and Stretchable Ag Nanowire/Carbon Nanotube Hybrid Conductors," Nanotechnology, 25(28), p. 285203.

- [29] Jo, H. S., An, S., Lee, J. G., Park, H. G., Al-Deyab, S. S., Yarin, A. L., and Yoon, S. S., 2017, "Highly Flexible, Stretchable, Patternable, Transparent Copper Fiber Heater on a Complex 3D Surface," NPG Asia Mater., 9(2), p. e347.
- [30] Hu, X., Krull, P., de Graff, B., Dowling, K., Rogers, J. A., and Arora, W. J., 2011, "Stretchable Inorganic-Semiconductor Electronic Systems," Adv. Mater., 23(26), pp. 2933–2936.
- [31] Liu, Y., Kolbakir, C., Hu, H., Meng, X., and Hu, H., 2019, "An Experimental Study on the Thermal Effects of Duty-Cycled Plasma Actuation Pertinent to Aircraft Icing Mitigation," Int. J. Heat Mass Transfer, 136, pp. 864–876.
- [32] Shahriari, E., and Varnamkhasti, M. G., 2014, "Nonlinear Optical and Electrical Characterization of Nanostructured Cu Thin Film," Superlattices Microstruct., 75, pp. 523–532.
- [33] Wang, T., Li, B., Ren, N., Huang, L., and Huang, L., 2019, "Influence of Al/Cu Thickness Ratio and Deposition Sequence on Photoelectric Property of ZnO/Al/Cu/ZnO Multilayer Film on PET Substrate Prepared by RF Magnetron Sputtering," Mater. Sci. Semicond. Process., 91, pp. 73–80.
- [34] Ko, Y. H., Kim, M. S., and Yu, J. S., 2012, "Controllable Electrochemical Synthesis of ZnO Nanorod Arrays on Flexible ITO/PET Substrate and Their Structural and Optical Properties," Appl. Surf. Sci., 259, pp. 99–104.
- [35] Lahiri, B., Dylewicz, R., La Rue, R. M. D., and Johnson, N. P., 2010, "Impact of Titanium Adhesion Layers on the Response of Arrays of Metallic Split-Ring Resonators (SRRs)," Opt. Express, 18(11), pp. 11202–11208.
- [36] Taylor, A. A., Cordill, M. J., Bowles, L., Schalko, J., and Dehm, G., 2013, "An Elevated Temperature Study of a Ti Adhesion Layer on Polyimide," Thin Solid Films, 531, pp. 354–361.
- [37] Bauccio, M. L., ed., 1993, ASM Metals Reference Book, ASM International, Materials Park, OH.